

Deposition of Titania Thin Films by a Peroxide Route on Different Functionalized Organic Self-Assembled Monolayers

Thomas P. Niesen,* Joachim Bill, and Fritz Aldinger

Max-Planck-Institut für Metallforschung and Institut für Nichtmetallische Anorganische Materialien, Universität Stuttgart, Pulvermetallurgisches Laboratorium, Heisenbergstrasse 5, D-70569 Stuttgart, Germany

Received November 20, 2000. Revised Manuscript Received February 5, 2001

Self-assembled monolayers (SAMs) on single-crystal Si wafers have been used as substrates for the deposition of oxide thin films. The organic surface has been shown to be effective for promoting the growth of films from aqueous solutions at temperatures below 100 °C. In the present study, the formation of a titanium complex in the presence of H₂O₂ is used to stabilize an otherwise spontaneously precipitating aqueous titanium solution. Uniform titania films have been formed at 80 °C on sulfonated SAMs, whereas hydroxyl and amine functionalities led to inhomogeneous coatings. The films were characterized by a variety of techniques, including ellipsometry, RBS, AFM, SEM, and TEM, to determine the thickness, topography, microstructure, and chemical composition of the films. An electronegativity–pH diagram is used to explain how the composition of the deposition solution is reflected in the final thin film, both for the present films and for titania films reported earlier in the literature. Finally, the current understanding of the film formation mechanism is discussed.

I. Introduction

Titania is well-known for its high refractive index, permittivity, and transmittance of visible light. These properties make it suitable for many applications such as use in dielectric layers in microelectronic devices,¹ oxygen sensors,² and high-efficiency catalysts.³ A number of vapor-phase deposition techniques have been previously used to form high-quality TiO₂ films. However, these techniques have several shortcomings, such as expensive vacuum equipment, the need to heat the substrates to crystallize the films, and the limitations of line-of-sight deposition. Sol–gel solution routes with alkoxide precursors have been successfully used to coat films on complex-shaped substrates, but postdeposition treatment at temperatures typically >400 °C is required to form thermodynamically stable phases.⁴

As a consequence, there has been a growing interest in low-temperature thin film deposition techniques from aqueous solutions during the past decade.⁵ A more recent, bioinspired strategy in this context is to focus on substrates previously coated with organic self-assembled monolayers (SAMs). SAMs are ordered molecular assemblies formed by the chemical adsorption of an active surfactant on a solid surface. It is believed that the functional surfaces can behave analogously to

proteins in biological systems to promote the deposition of an inorganic phase: SAMs have been shown to be effective surfaces for promoting the formation of oxide thin films from aqueous solutions at temperatures below 100 °C, in cases where film formation was not possible without an underlying SAM. The oxide films, including nanocrystalline TiO₂,^{6,7} ZrO₂,⁸ V₂O₅,⁹ ZnO,¹⁰ Fe₃O₄,¹¹ and SnO₂,¹² are adherent and microstructurally uniform.

In earlier depositions of titania thin films on SAMs from aqueous solutions,⁶ highly acidic solutions, such as 0.5 M TiCl₄/6 N HCl, were necessary to prevent the solution from spontaneous bulk precipitation. Films with a typical thickness of <60 nm could be formed in 2–4 h on sulfonated SAMs. The films consisted of densely packed, randomly oriented TiO₂ (anatase) crystals that were 2–4 nm in diameter. Later, Huang et al.¹³ adapted this procedure to deposit titania thin films on SAM-coated industrial glass. Patterned titania films

* Corresponding author. Present address: Siemens AG, Corporate Technology, D-81739 München, Germany.

(1) Burns, G. P. *J. Appl. Phys.* **1989**, *65*, 2095.
 (2) Nabavi, M.; Doeuff, S.; Sanchez, C.; Livage, J. *Mater. Sci. Eng.* **1989**, *B3*, 203.
 (3) Carlson, T.; Griffin, G. L. *J. Phys. Chem.* **1980**, *84*, 5896.
 (4) Brinker, C. J.; Scherer, G. W. *Sol–Gel Science: The Physics and Chemistry of Sol–Gel Processing*; Academic Press: San Diego, CA, 1990.
 (5) Niesen, T. P.; De Guire, M. R. *J. Electroceram.*, in press.

(6) Shin, H.; Collins, R. J.; De Guire, M. R.; Heuer, A. H.; Sukenik, C. N. *J. Mater. Res.* **1995**, *10*, 692.

(7) Baskaran, S.; Song, L.; Liu, J.; Chen, Y. L.; Graff, G. L. *J. Am. Ceram. Soc.* **1998**, *81*, 401.

(8) Agarwal, M.; De Guire, M. R.; Heuer, A. H. *J. Am. Ceram. Soc.* **1997**, *80*, 2967.

(9) Niesen, T. P.; Wolff, J.; Bill, J.; De Guire, M. R.; Aldinger, F. In *Organic–Inorganic Hybrid Materials II*; Klein, L. C., Francis, L. F., De Guire, M. R., Mark, J. E., Eds.; MRS Symposium Proceedings; Materials Research Society: Warrendale, PA, 1999; Vol. 576, p 197.

(10) De Guire, M. R.; Niesen, T. P.; Supothina, S.; Wolff, J.; Bill, J.; Sukenik, C. N.; Aldinger, F.; Heuer, A. H.; Rühle, M. *Z. Metallk.* **1998**, *89*, 758.

(11) Maiti, M. M. S. Thesis, Case Western Reserve University, Cleveland, OH, 1994.

(12) Supothina, S.; De Guire, M. R. *Thin Solid Films* **2000**, *371*, 1.

(13) Huang, D.; Xiao, Z. D.; Gu, J. H.; Huang, N. P.; Yuan, C. W. *Thin Solid Films* **1997**, *305*, 110.

have been formed after photolysis and oxidation of thioacetate-terminated SAMs through a mask (i.e., to sulfonated areas), followed by immersion in TiCl_4/HCl solution, which left the non-oxidized areas uncoated by titania.¹⁴ Koumoto et al.¹⁵ deposited TiO_2 from hexafluorotitanate solution (following Deki et al.¹⁶) using a patterned phenyltrichlorosilane SAM as the substrate. Areas where the SAM had been removed via Si–C bond photocleavage were coated by a film, while the deposits on the SAM could be easily removed by ultrasonication. Baskaran et al.⁷ used an aqueous titanium lactate solution to deposit titania films on sulfonated SAMs and plastic surfaces with high deposition rates.

In this paper, we describe the preparation of titania thin films deposited from aqueous solutions stabilized by complexation with an inorganic ligand. In the presence of hydrogen peroxide and at a $\text{pH} < 1$, stable monomolecular hydrated $[\text{TiO}_2]^{2+}$ is formed through the η^2 coordination (side-on) of O_2^{2-} to Ti^{4+} .^{17,18} In the range $1 < \text{pH} < 3$, deprotonation and condensation of the cation led to slow deposition of an amorphous precipitate of peroxotitanium hydrate $\text{TiO}_3 \cdot 1.5\text{H}_2\text{O}$. Above $\text{pH} = 3$, rapid neutralization and condensation of anionic species occurred. Cathodic electrodeposition (i.e., pH shift by electrogenerated base formation) from such a solution was reported by Zhitomirsky and Gal-Or.¹⁹ The amorphous precipitate was transformed to anatase by heat treatment at 400°C . In contrast, films have been formed by electroless deposition under acidic conditions ($\text{pH} < 1$) in the present work. The influence of different functionalized SAMs on the nucleation and growth of the films was investigated.

II. Experimental Section

Film Deposition. The substrates were p-type {001} single-crystal Si wafers, polished on one side and approximately $10\text{ mm} \times 10\text{ mm}$ in size. These wafers were cleaned and oxidized in piranha solution (70 vol % of H_2SO_4 , 30 vol % of 30 wt % H_2O_2 aqueous solution). The wafers were then dipped into 1,1'-bicyclohexyl solution containing 1 vol % of the surfactant (trichlorosilylhexadecane thioacetate or -nitrile and ω -heptadecyltrichlorosilane) at room temperature under inert atmosphere for several hours, during which time the SAM formed spontaneously. Finally, the wafers were thoroughly washed in chloroform to remove all traces of excess surfactant. (Further details of the synthesis of the SAMs on Si can be found elsewhere.^{20–22})

To convert the thioacetate into a sulfonate ($-\text{SO}_3\text{H}$) functionality, the wafers were immersed in oxone (potassium hydrogenmonopersulfate, Merck) for a minimum of 4 h at room temperature.²¹ The nitrile functionality was transformed into an amino ($-\text{NH}_2$) functionality by reduction with a saturated solution of lithium aluminum hydride in diethyl ether for 15 h at room temperature and subsequent quenching with 5 vol % hydrochloric acid.²⁰ The vinyl group of ω -heptadecenyl-

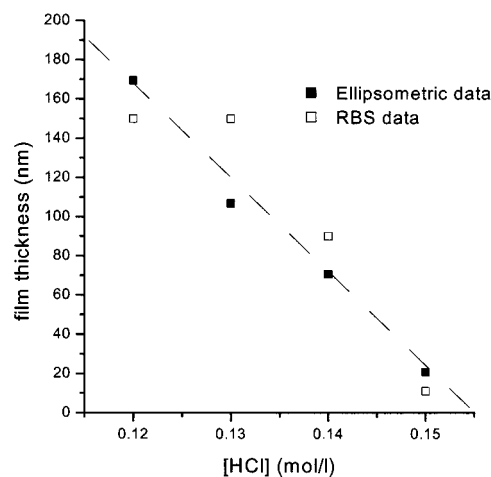


Figure 1. Dependence of film thicknesses on the acid concentration used (10 mM TiO_2^{2+} , 4 h of deposition at 80°C , horizontal orientation).

trichlorosilane was hydroborated with a boran–tetrahydrofuran complex for 2 h and subsequently quenched to an $-\text{OH}$ functionality with 30% $\text{H}_2\text{O}_2/0.1\text{ N NaOH}$.²² XPS and contact angle measurements were used to confirm the success of these conversions.

Freshly distilled TiCl_4 (0.1 mol) was added dropwise to an ice-cooled aqueous solution containing H_2O_2 (0.2 mol). Stock solutions of 10 mM TiO_2^{2+} and 0.12–0.15 N HCl (excluding acid from TiCl_4 hydrolysis) were prepared from this solution and hydrochloric acid. The SAM-coated substrates were immersed in 10-mL aliquots of this solution, covered, and then placed in an oil bath at 80°C . Samples were immersed for between 4 and 6 h, in the horizontal or vertical orientation. (No visible bulk precipitation occurred during such depositions.) Finally, the samples were washed with distilled water, ultrasonicated, and dried with a stream of dry argon gas. Control experiments were done with piranha-oxidized Si wafers (i.e., without SAMs). Precipitate that was formed in the deposition solution after it was aged at 80°C for 3 days was collected and air-dried.

Film Characterization. The films were analyzed using X-ray photoelectron spectroscopy (Perkin-Elmer ESCA 5400). Film thicknesses were measured using ellipsometry and RBS (NEC 5SDH). A Digital Instruments Nanoscope III AFM was used in tapping mode; scans were taken in air at room temperature. A Zeiss DSM 982 Gemini field-emission scanning electron microscope (SEM) and a JEOL JEM 2000FX instrument (TEM) were used to characterize the microstructure of the films. TEM samples were prepared following ref 23. The visualized section of the film is found on top of epoxy as an artifact of the TEM sample preparation. Electron diffraction was employed for phase identification. Grazing-incidence X-ray diffraction patterns were recorded on a Siemens D5000 instrument.

III. Results

Film Growth Conditions. Adherent titania films were formed on sulfonated SAMs from 10 mM TiO_2^{2+} solutions with added 0.12–0.15 N HCl at 80°C in 4 h. In these experiments, silicon substrates were oriented horizontally during deposition. The films showed a uniform interference color. Ellipsometric and RBS investigations revealed a roughly linear dependence of the film thicknesses on the acid concentration used (Figure 1). Lower acid concentrations led to visible bulk precipitation during deposition. Even when no visible bulk

(14) Collins, R. J.; Shin, H.; De Guire, M. R.; Heuer, A. H.; Sukenik, C. N. *Appl. Phys. Lett.* **1996**, *69*, 860.

(15) Koumoto, K.; Seo, S.; Sugiyama, T.; Seo, W. S. *Chem. Mater.* **1999**, *11*.

(16) Deki, S.; Aoi, Y.; Hiroi, O.; Kajinami, A. *Chem. Lett.* **1996**, *1996*, 433.

(17) Mühlebach, J.; Müller, K.; Schwarzenbach, G. *Inorg. Chem.* **1970**, *9*, 2381.

(18) Rotzinger, F. P.; Grätzel, M. *Inorg. Chem.* **1987**, *26*, 3704.

(19) Zhitomirsky, I.; Gal-Or, L. *J. Eur. Ceram. Soc.* **1996**, *16*, 819.

(20) Balachander, N.; Sukenik, C. N. *Langmuir* **1990**, *6*, 1621.

(21) Collins, R. J.; Sukenik, C. N. *Langmuir* **1995**, *11*, 2322.

(22) Wasserman, S. R.; Tao, Y. T.; Whitesides, G. M. *Langmuir* **1989**, *5*, 1074.

(23) Strecker, A.; Salzberger, U.; Mayer, J. *Prakt. Metallogr.* **1993**, *30*, 482.

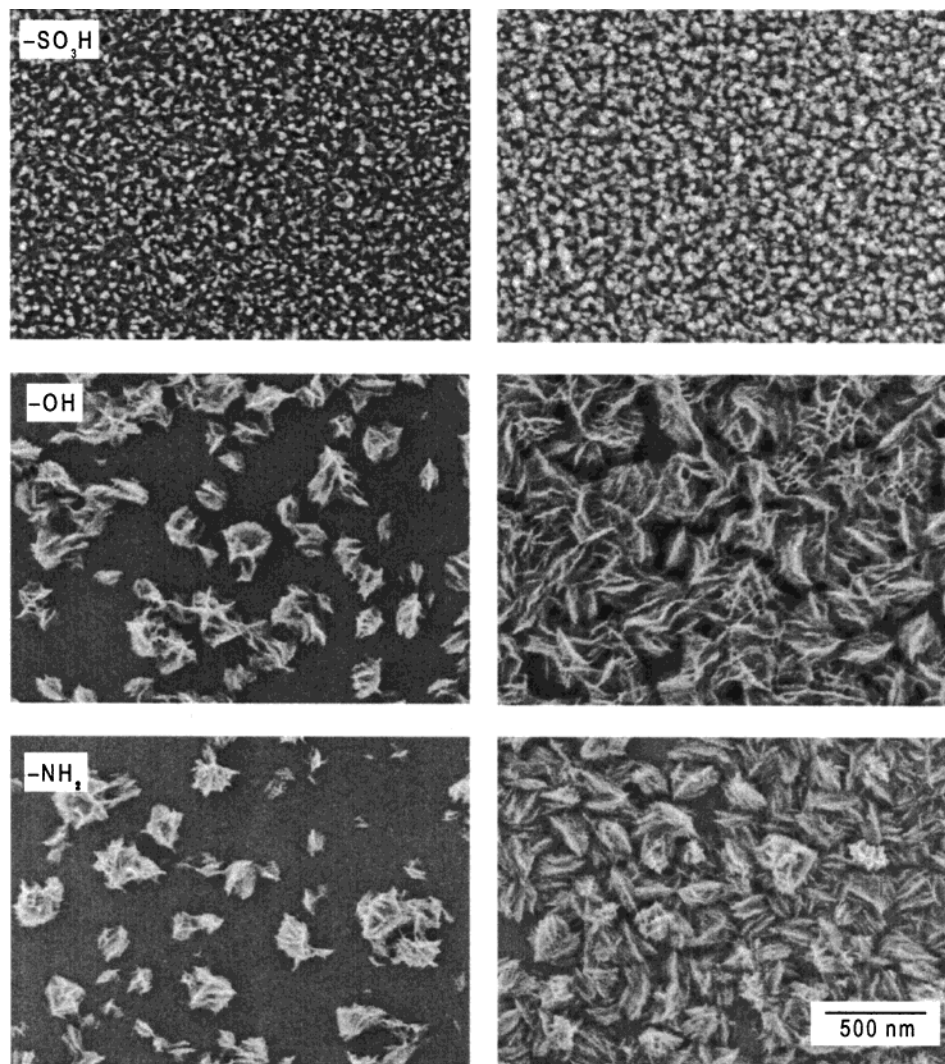


Figure 2. SEM micrographs of TiO_2 thin films on different functionalized SAMs after 4 (left) and 6 h (right) of deposition at 80°C .

precipitation occurred during film growth, film quality was improved by vertical orientation of the substrates. However, films formed in this orientation were found to be notably thinner than those formed in the horizontal arrangement, e.g., 50 nm in contrast to 100 nm (4 h of deposition with 0.14 N added HCl).

In the XPS spectra, signals for Ti (464.7 and 459.0 eV) and O (530.8 eV) were detected. (Peaks were calibrated using the characteristic C1s peak at 284.6 eV.) If sulfonated SAMs were used, complete coverage by the film could be inferred from the absence of Si signals. Both the shoulder of the O1s peak and the ratio of the XPS oxygen and titanium signals, which exceeded the stoichiometry of 2:1 for TiO_2 , indicate the formation of hydrated oxide. RBS curve fits evidenced the incorporation of 0.4–0.8 equiv of H_2O per mol TiO_2 , in agreement with the XPS measurements.

Influence of Different SAMs. Different functionalized SAMs were used under otherwise identical experimental conditions. Figure 2 shows SEM micrographs of films deposited on $-\text{SO}_3\text{H}$, $-\text{NH}_2$, and $-\text{OH}$ functionalities, for 4 and 6 h of deposition at 80°C . On sulfonated SAMs, a uniform film of densely packed particles was formed in 4 h. The morphology of the films did not change during further film growth. In contrast,

hydroxyl and amino functionalities led to islandlike growth. These islands were 70–200 nm in size after 4 h, and uncoated substrate (i.e., the SAM) was found between them. The islands seemed to grow together if the deposition was continued, so that the final films consisted of domains. Such films were partially optically opaque, whereas films on sulfonated SAMs were always specularly reflecting. No attempts to measure the adherence of the films were made; however, all samples were ultrasonicated before being dried to remove loosely attached particles. Control experiments showed that films were not formed on piranha-oxidized silicon wafers.

Films Deposited on Sulfonated SAMs. Atomic force microscopy was used to analyze the surface topography of a titania film deposited in 6 h from 10 mM TiO_2^{2+} and 0.14 N HCl at 80°C on a sulfonated SAM (Figure 3). The AFM image reveals a dense packing of agglomerates that are 50–100 nm in width and had height variations of 50–60 nm. Such topography is typical for the whole specimen, and similar topographies were reproduced in other samples. The statistical roughness parameter remained lower than the height variations ($\text{rms} = 15\text{--}18$ nm, depending on the investigated area), supporting the idea that the

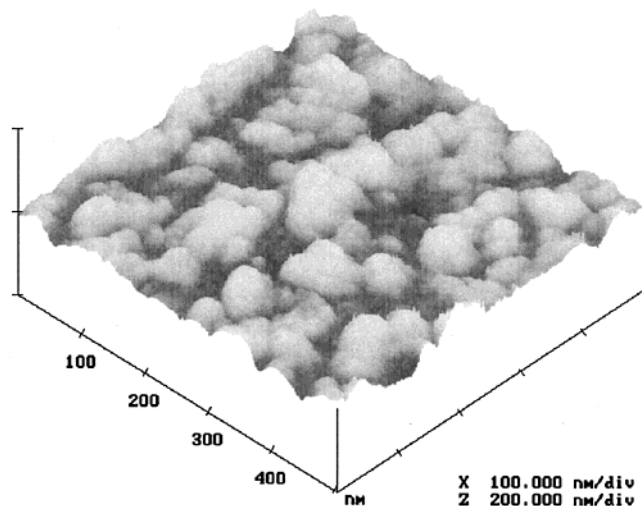


Figure 3. AFM image of a titania thin film on sulfonated SAM, deposited in 6 h at 80 °C, indicating roughness on a submicron scale.

coating's topography is very uniform. SEM micrographs of the same specimen are consistent with the AFM results. Films that had been annealed at 300 or 500 °C for 2 h in air showed no significant difference in SEM micrographs compared to those of the as-deposited films (Figure 4).

Cross-sectional TEM was used to investigate the microstructure of the as-deposited films. Figure 5 shows a micrograph of the specimen previously investigated by AFM (see above). The micrograph indicates a nanocrystalline and pore-free film that is 55–75 nm thick. The height variations are consistent with the previously described AFM and SEM results. The crystallites were identified as anatase from the lattice fringe spacings (Table 1).

Precipitate that was formed after the solution was aged for 3 days at 80 °C was found to be X-ray

Table 1. Electron and X-ray Diffraction Pattern Analysis of As-Deposited and Annealed TiO₂ Film^a

measured <i>d</i> spacing (nm)	electron diffraction	GI XRD ^b	X-ray powder diffraction pattern of anatase (JCPDS file no. 21-1272)		
			<i>d</i> (nm)	rel. intensity	{ <i>h k l</i> }
0.356		0.349	0.352	100	101
			0.243	10	103
			0.238	20	004
			0.233	10	112
0.187		0.189	0.189	35	200
			0.170	20	105
			0.167	20	211
			0.149	4	213
0.146			0.148	14	204
			0.128	2	107

^a For the electron diffraction pattern, the camera constant was calibrated using the Si substrate as an internal standard. ^b After annealing for 2 h at 500 °C in air.

amorphous (data not shown). Likewise, diffraction peaks were absent in grazing incidence XRD of as-deposited films, whereas the GI XRD pattern showed the most intense peaks of the anatase structure after the samples were annealed at 500 °C (Table 1), indicating further crystallization and grain growth during annealing.

IV. Discussion

Hydrolysis of Metal Salts in Aqueous Solution.

The aqueous chemistry of a metal salt is, in general, much more complicated than the hydrolysis of the corresponding metal alkoxide. Several monomeric or condensed species exist simultaneously in the aqueous medium, depending on parameters such as pH, concentration, and temperature. The structure and composition of the solid phases depend on the presence of anions even when they do not seem to be involved in the chemical process. For example, whereas the thermohydrolytic precipitation from sulfuric acid solutions of

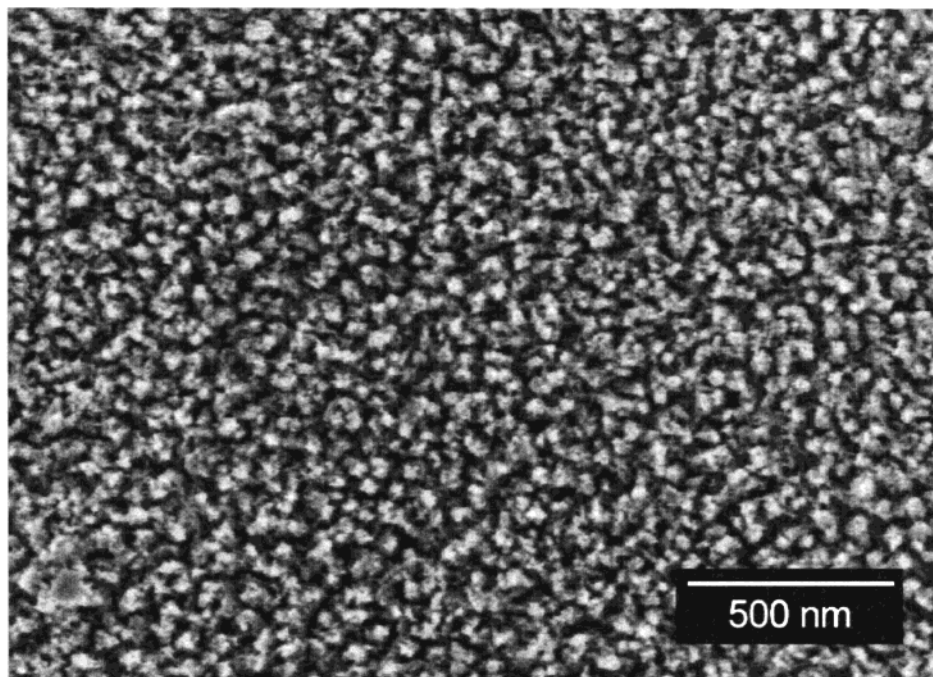


Figure 4. SEM micrograph of a titania thin film on sulfonated SAM, deposited in 6 h at 80 °C, after 2 h of annealing at 500 °C in air.

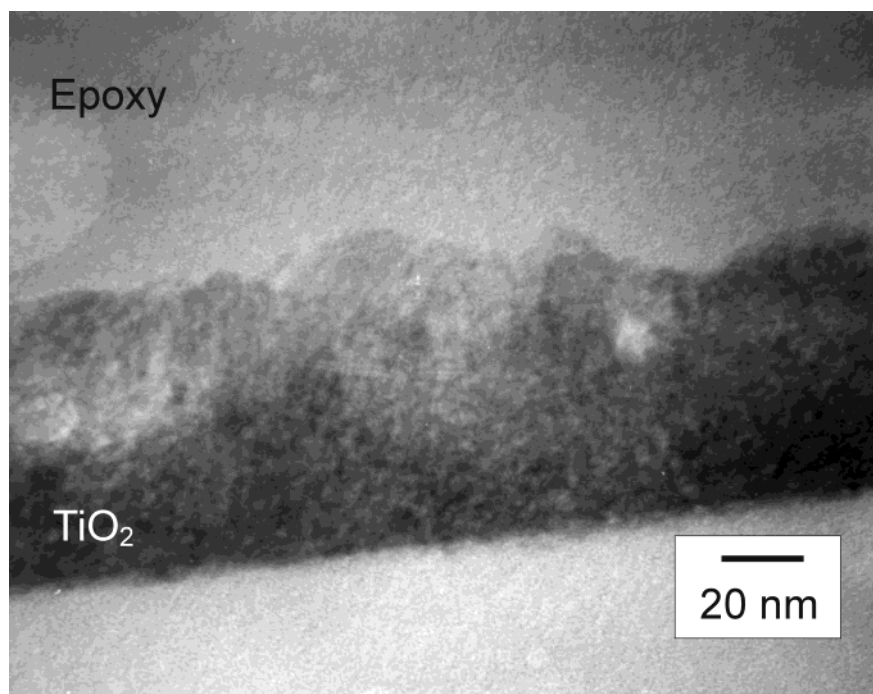
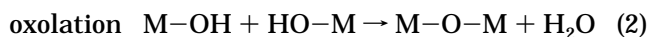
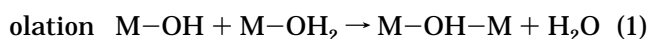


Figure 5. Cross-sectional TEM micrograph of a titania film on sulfonated SAM, deposited in 6 h at 80 °C.

titanium salts produces only anatase, the formation of both anatase and rutile is possible from hydrochloric or nitric acid solutions, depending on the acid concentration.²⁴ Henry et al.²⁵ provided a quantitative relationship between hydrolysis and electronegativity (based on a so-called partial charge model) that is used here to explain how thin titania films reflect the chemical natures of their aqueous deposition solutions.

In general, the condensation of hydrolyzed metal ions follows two main mechanisms, olation and oxolation, leading to the formation of ol and oxo bridges, respectively.



The stability of the M–OH bond and the occurrence of olation rather than oxolation is found to depend on the electronegativity of the solvated metal ion.²⁵ Briefly, hydrolyzed cations with electronegativities χ_M between two critical values χ_{OH}^* and χ_{O}^* condense both through olation and through oxolation, leading to hydrous oxide precipitation (e.g., Ti), whereas those with $\chi_M < \chi_{\text{O}}^*$ condense only through olation (leading to hydroxide precipitation, e.g., Zn) and those with $\chi_M > \chi_{\text{OH}}^*$ condense only through oxolation (leading to poly-acid formation, e.g., V).

The first hydrolysis product of a titanium salt, $[\text{Ti}(\text{OH})(\text{OH}_2)_5]^{3+}$, deprotonates spontaneously and then undergoes intramolecular oxolation to the monomeric $[\text{TiO}(\text{OH}_2)_5]^{2+}$ cation and olation to the neutral dimer $[\text{Ti}_2\text{O}_2(\text{OH})_4(\text{OH}_2)_4]$.²⁵ Although the formation of an octameric $[\text{Ti}_8\text{O}_8(\text{OH})_{12}]^{4+}$ polycation has been re-

ported,²⁶ linear-chain polycondensation seems to be energetically favored (in contrast to the case for the bigger Zr^{4+} ions²⁷). The formation of different titania polymorphs can be explained by the occurrence of deoxolation steps (i.e., $\text{O}=\text{Ti}-\text{OH}_2 \rightarrow \text{HO}-\text{Ti}-\text{OH}$) during the further condensation of the octahedrons: Olation of the dimers in *equatorial* positions, followed by deoxolation and subsequent oxolation between the linear chains, leads to the rutile structure. In contrast, if the deoxolation occurs *before* the olation, the dimers condense in *apical* positions, leading to the anatase structure.²⁵

Role of Complexants during Hydrolysis. As noted before, complexation by anions has an important influence on the formation of the condensed phases. At a given hydrolysis ratio, complexation occurs if the electronegativity χ_p of the resulting metal complex is higher than the anion's electronegativity χ_x but lower than the electronegativity of the fully protonated anionic species χ_{HX} .²⁵ If stable complexes are formed, monovalent anions transform the network and lead to basic salt precipitation (i.e., including the anion in the precipitate). Multivalent anions can be eliminated through ionic dissociation if the electronegativity of the metal species is lower than that of a partially protonated anion ($\chi_x \leq \chi_p \leq \chi_{\text{HX}}$). In such a case, the resulting precipitate remains free of anions.

According to this analysis, electronegativity–pH diagrams are direct guides in predicting whether complexation occurs. To compute the electronegativity of the peroxy and hydroperoxy anions in aqueous solution, their first coordination sphere has to be included. As no data are available for the solvated anions, solid compounds were used as a reference. Coordination of

(24) Bekkerman, L. I.; Dobrovolskii, I. P.; Ivakin, A. A. *Russ. J. Inorg. Chem.* **1976**, *21*, 223.

(25) Henry, M.; Jolivet, J. P.; Livage, J. *Struct. Bonding* **1992**, *77*, 153.

(26) Einaga, H.; Komatsu, Y. *J. Chem. Soc., Dalton Trans.* **1981**, 2443.

(27) Singhal, A.; Toth, L. M.; Lin, J. S.; Affholter, K. *J. Am. Chem. Soc.* **1996**, *118*, 11529.

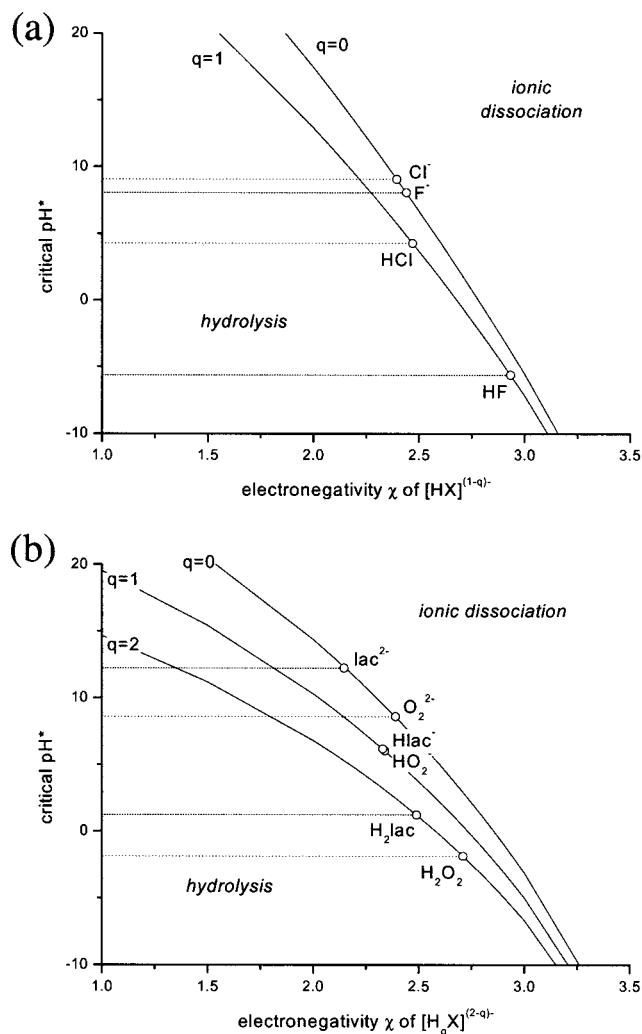


Figure 6. Electronegativity–pH diagram for complexation of Ti^{4+} by the q -protonated anion X^{n-} . Stable complexes are formed between the curves, whereas outside the curves, hydrolysis or ionic dissociation occurs (see text for details; $\text{lac} = \text{C}_3\text{H}_4\text{O}_3^{2-}$).

the peroxide anion by eight water molecules was found in $\text{Na}_2\text{O}_2 \cdot 8 \text{H}_2\text{O}$,²⁸ whereas the hydroperoxo anion coordinates with one water molecule in $\text{LiHO}_2 \cdot \text{H}_2\text{O}$.²⁹ The calculated results (Figure 6; see appendix for derivation of the data) indicate the formation of a stable peroxy complex even under strong acidic conditions, in agreement with experiment.^{17,18} Mühlebach et al.¹⁷ suggested the formation of amorphous peroxotitanium hydrate $\text{TiO}(\text{O}_2) \cdot a\text{q}$ at $\text{pH} \approx 1-3$. Deposits by electro-generated base have also been reported to consist of peroxotitanium hydrate.³⁰ The formation of such a “basic salt” is consistent with the analysis based on the calculated electronegativities, i.e., $\chi_{\text{HX}} \leq \chi_q \leq \chi_{\text{H}_2\text{X}}$ ($2.3 \leq 2.7 \leq 2.7$ for $\text{M} = [\text{Ti}(\text{O}_2)\text{OH}(\text{H}_2\text{O})_3]^+$). Therefore, it seems plausible that the amorphous part in the present films is formed by peroxotitanium hydrate or, after thermal decomposition at the deposition temperature, by titanium oxide hydrate. The formation of anatase nanocrystallites seems to be related to the deposition mechanism (see below).

Such electronegativity–pH diagrams are also helpful to understand how and why different anions influenced the TiO_2 thin film deposition from aqueous solution in previously published work. According to our calculations, complexation of solvated titanium ions by Cl^- would only be possible under neutral conditions (i.e., under conditions where hydrolysis and complexation already dominate). Others have shown experimentally that chlorine can only enter the inner coordination sphere of titanium if there is insufficient water for coordination.³¹ Shin et al.⁶ found that their films deposited from 0.5 M $\text{TiCl}_4/6 \text{ N HCl}$ to consist of densely packed, randomly oriented anatase crystallites surrounded by a thin amorphous layer. The films contained only a small amount of chlorine (typically less than 1 wt %), in agreement with the instability of the chlorine complexes.³² According to the XPS spectra of the films, the oxygen-to-titanium ratio is close to 2:1,⁶ indicating the high stoichiometry of a product formed from highly acidic conditions. (Films deposited by Huang et al.^{13,33} under similar conditions showed significant Si signals in their XPS spectra; therefore, the reported oxygen-to-titanium ratio of $\sim 3:1$ includes oxygen from the substrate.)

In contrast to chlorine, stable fluorine complexes should also be formed under acidic conditions (Figure 6a), in agreement with the experimental observations.¹⁶ Therefore, the LPD films typically contain a significant amount of fluorine: 7.2 mass % of F was found in TiO_2 powder deposited from the LPD solution.³⁴ However, the fluorine content seems to favor the crystallinity of the film, as Koumoto et al.¹⁵ found highly (004) orientation of their anatase thin films after deposition from an ammonium titanium fluoride solution even at $\text{pH} \approx 2.9$.

By calculation, the bivalent lactate anion leads to stable complexes for $\text{pH} \approx 1-12$ (Figure 6b), which is in good agreement with the precipitation and film-formation conditions reported by Baskaran et al.⁷ They found a mixture of anatase and the less compact structure type TiO_2 (B)³⁵ in the precipitates, whereas the films were predominantly crystalline TiO_2 (B) with amorphous TiO_2 as a minor phase. (Films on polycarbonate consisted of amorphous, hydrated TiO_2 only.) On the basis of an electronegativity analysis, because $\chi_{\text{X}} \leq \chi_q \leq \chi_{\text{HX}}$ ($2.1 \leq 2.1 \leq 2.3$ for $[\text{Ti}(\text{C}_3\text{H}_4\text{O}_3)_2(\text{OH})_2]^{2-}$), the lactate anion can be eliminated during film growth, in agreement with experiment.

Deposition Mechanism. Heterogeneous nucleation and surface-directed growth is suggested to be the principal deposition mechanism in the liquid-phase deposition process, strongly supported by the orientation of the films.¹⁵ The same argument holds for goethite films deposited on SAMs under limited experimental conditions.^{36,37} It was suggested that a substrate with

(31) Hildenbrand, V. D.; Fuess, H.; Pfaff, G.; Reynders, P. *Z. Phys. Chem.* **1996**, *194*, 139.

(32) Shin, H.; De Guire, M. R.; Heuer, A. H. *J. Appl. Phys.* **1998**, *83*, 3311.

(33) Xiao, Z.; Gu, J.; Huang, D.; Lu, Z.; Wei, Y. *Appl. Surf. Sci.* **1998**, *125*, 85.

(34) Kishimoto, H.; Takahama, K.; Hashimoto, N.; Aoi, Y.; Deki, S. *J. Mater. Chem.* **1998**, *8*, 2019.

(35) Marchand, R.; Brohan, L.; Tournoux, M. *Mater. Res. Bull.* **1980**, *15*, 1129.

(36) Rieke, P. C.; Marsh, B. D.; Wood, L. L.; Tarasevich, B. J.; Liu, J.; Song, L.; Fryxell, G. E. *Langmuir* **1995**, *11*, 318.

(28) Hill, G. S.; Holah, D. G.; Kinrade, S. D.; Magnuson, V. R.; Polyakov, V.; Sloan, T. A. *Can. J. Chem.* **2000**, *75*, 46.

(29) Cohen, A. J. *J. Am. Chem. Soc.* **1952**, *74*, 3762.

(30) Zhitomirsky, I. *Mater. Lett.* **1998**, *33*, 305.

suitable surface chemistry induces film formation at levels of supersaturation that do not sustain homogeneous nucleation.³⁸

As is discussed in more detail elsewhere,^{39,40} we believe that films on functionalized SAMs can also be formed via attachment to the substrate of nanosized particles formed in the bulk solution. For a particle attachment mechanism, the net attraction results from the summation of electrostatic, van der Waals, and hydration interactions. When the diameter of the particles exceeds a size of ~ 10 nm, these forces will be negligibly small.⁴¹ Therefore, such particles do not contribute to the film growth, in agreement with the film's microstructure. Whereas van der Waals forces are always attractive and hydration forces repulsive, the electrostatic term depends on the functionalization of the surface. For a positively charged titania colloidal particle, the sulfonate group—deprotonated even in acidic solution—leads to attraction, whereas the protonated amine group leads to repulsion. As a consequence, the net attraction is highest for sulfonated SAMs, in agreement with the experimental results. Whereas film formation starts early on sulfonated SAMs, for both of the other investigated functionalities, the induction time is large. Heterogeneous nucleation, which competes with the particle attachment mechanism, could explain the initially islandlike growth on the latter SAMs. It should be pointed out that films were not formed directly on piranha-oxidized silicon (i.e., also hydroxyl-terminated), indicating the higher reactivity of the SAM's headgroup or the higher density of the functional group in the SAM. Others^{6,7} have also reported that no films were formed on the native surface oxide or on wafers that had been treated to optimize the number of surface OH groups, with the notable exception of the LPD films.^{15,16}

In contrast to the present films on sulfonated SAMs, titania films deposited from strong acidic aqueous solution (0.5 M TiCl₄/6 M HCl) showed a background roughness on a finer scale (< 10 nm).⁴⁰ Such surface roughness is in agreement with the size of the nanocrystallites that form the films, whereas the surface morphology seems to be influenced by additional factors in the present work. Islandlike growth in the very beginning of the deposition might contribute to the topography of the final film. However, AFM investigations of LPD-grown titania thin films showed a comparable microstructure, with particles ~ 50 nm in diameter (by heterogeneous growth mode) and some large particles (> 500 nm) that are considered to be formed in the bulk of the solution.³⁴ Likewise, Xiao et al.⁴² observed particles of ~ 100 nm in size and ~ 12 nm in height in AFM micrographs of titania films grown on sulfonated

SAMs, whereas mixed $-\text{SH}$ and $-\text{SO}_3\text{H}$ monolayers led to particle sizes up to 200 nm.

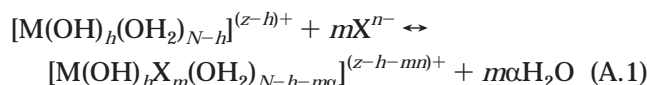
V. Conclusions

Thin titania films were successfully deposited from an aqueous titanium peroxide solution at 80 °C. Calculated electronegativity–pH diagrams proved to be useful tools for predicting and understanding the chemistry of the formed condensed phases. The predominant effect of the sulfonic acid surface group in promoting the film growth has been shown, which is in agreement with several other reports^{8,36,43,44} and with the suggested role of acidic groups in protein structures in biomineralization.⁴⁵ The presence of an uncharged or positively charged surface does not generally exclude film formation. However, changes in deposition mechanism occur that led here to nonuniform, partially opaque films under identical experimental conditions. Future investigations are necessary to fully understand the deposition mechanisms.

Acknowledgment. The authors thank D. Cantarutti, H. Labitzke, U. Salzberger, Prof. J. Schneider, Dr. T. Wagner, Prof. M. Hu (ORNL, Oakridge, TN), Dr. U. Sampathkumaran, and A. McIlwain (CWRU, Cleveland, OH) for providing support with characterization of the films and Wacker Chemitronics for supplying silicon wafers. Helpful discussions with Prof. M. R. De Guire (CWRU, Cleveland, OH) are gratefully acknowledged. This work was financially supported by the Deutsche Forschungsgemeinschaft (Al 384/22-1/2) and the U.S. National Science Foundation (Grant DMR 9803851 to M.R.D.)

Appendix

The starting point for computing the pH ranges for complexation of the hydrolyzed metal cation M^{z+} by the anion X^{n-} is the reaction



where z is the oxidation state of the metal, h is the hydrolysis ratio, N is the coordination number, n is the valency of the anion, m is the number of coordinated anions, and α is the coordination mode of the anion ($\alpha = 1$ for monodentate ions and $\alpha = 2$ for bidentate anions).

Briefly, the mean electronegativity of the complexed metal species χ_p has to be equalized with the mean electronegativity χ_q of the q -protonated form of the anion X^{n-} . If charge conservation within the complexed species is applied, a critical hydrolysis ratio h_q^* can be calculated from this equation, which is converted into a critical pH value, pH_{q^*} . A detailed calculation is presented in ref 25.

(37) Rieke, P. C.; Wiecek, R.; Marsh, B. D.; Wood, L. L.; Liu, J.; Song, L.; Fryxell, G. E.; Tarasevich, B. J. *Langmuir* **1996**, *12*, 4266.

(38) Bunker, B. C.; Rieke, P. C.; Tarasevich, B. J.; Campbell, A. A.; Fryxell, G. E.; Graff, G. L.; Song, L.; Liu, J.; Virden, J. W.; McVay, G. L. *Science* **1994**, *264*, 48.

(39) Shin, H.; Agarwal, M.; De Guire, M. R.; Heuer, A. H. *Acta Mater.* **1998**, *46*, 801.

(40) Niesen, T. P.; De Guire, M. R.; Bill, J.; Aldinger, F.; Rühle, M.; Fischer, A.; Jentoft, F. C.; Schlögl, R. *J. Mater. Res.* **1999**, *14*, 2464.

(41) Sampathkumaran, U.; Supothina, S.; Wang, R.; De Guire, M. R. In *Mineralization in Natural and Synthetic Biominerals*; Li, P., Calvert, P., Levy, R. J., Kokubo, T., Scheid, C. R., Eds.; MRS Symposium Proceedings; Materials Research Society: Warrendale, PA, 2000; Vol. 599, 177–188.

(42) Xiao, Z.; Su, L.; Gu, N.; Wei, Y. *Thin Solid Films* **1998**, *333*, 25.

(43) Meldrum, F.; Flath, J.; Knoll, W. *J. Mater. Chem.* **1999**, *9*, 711.

(44) Nagtegaal, M.; Stroeve, P.; Enslin, J.; Gütlich, P.; Schurrer, M.; Voit, H.; Flath, J.; Käshammer, J.; Knoll, W.; Tremel, W. *Chem. Eur. J.* **1999**, *5*, 1331.

(45) Addadi, L.; Weiner, S. *Angew. Chem., Int. Ed. Engl.* **1992**, *31*, 153.

The final function of χ_q is

$$\text{pH}_q^* = 78.057 - 28.571 \times \frac{\chi_q(\Delta + 5.732\alpha + 2.064q) - 4.071(3.507\alpha + 2.064q)}{\Delta + (1.408\alpha + 0.507q)\chi_q - (3.507\alpha + 2.064q)} \quad (\text{A.2})$$

with

$$\Delta = z - 2.225N - (4.071 - \chi_M^0)/(1.36\sqrt{\chi_M^0})$$

Equation A.2 was used to calculate the data for Ti^{4+} cations with $z = 4$, $N = 6$, and $\chi_M^0 = 1.32$ (Figure 6).

The mean electronegativities of all molecular species were calculated from the electronegativities of the elements according to the partial charge model by the equation

$$\chi = \frac{\sum_i \sqrt{\chi_i^0} + 1.36z}{\sum_i \frac{1}{\sqrt{\chi_i^0}}} \quad (\text{A.3})$$

CM001227W